A RFI PROCESSING OF MULTI-SCALE REINFORCEMENT FOR SURFACE PROTECTION OF CFRP

Ben Wang[a], Yugang Duan[a*], Dilmurat Abliz[a,b], Gerhard Ziegmann[b]
[1] State Key Lab for Manufacturing Systems Engineering, Xi'an Jiaotong University, Xi'an , Shaanxi Province, 710049, , PR China
[2] Institute of Polymer Materials and Plastics Engineering, Clausthal University of Technology, Clausthal-Zellerfeld, 38678, Germany
Keywords: RFI, Multi-scale, Surface protection, Compoiste process

ABSTRACT

This paper reports the development of a resin film infusion method achieving a protective surface by the accumulation of functional nanofiller on the composite surface. In this method, the fibrous preform was sealed by the filter paper and the sealant tape to form a confined region that avoids the expansion of nanofiller from the fibrous perform while also limiting the nanofiller flow along the thickness direction. Thus, nanofiller accumulates on the CFRP surface through filtration mechanisms. In this study, graphene was selected as a nanofiller for reinforcement of polymers owing to its superior conductivity and large specific surface area characteristics. The accumulation of graphene on the CFRP surface allowed high conductivity values (440 S/cm vs. 16 S/cm of CFRP) on the surface while also improving the thermal resistance of CFRP. The friction and wear behavior of the resulting composites were investigated on a running-in process test rig. Experimental results revealed that the accumulation graphene layer contributed to improve the tribological properties of CFRP.

1 INTRODUCTION

At present, because of their potential for reducing weight, composites are being proposed for widespread use in the principal structures of new-generation facilities, such as aircraft, automobile and so on [1, 2]. Recent studies have highlighted the safety of these facilities that natural events can cause severe loss of containment, which triggering fatigue failure, toxic dispersion, fires or explosions with potentially severe consequences.

To guarantee the safety and ability of these composite facilities, it demands to endow the surface protection for the composite to commit these natural threats, such as radiation, lightning, friction, icing and flame. A plentiful researches have been adopted to incorporate the functional nanofiller with the resin matrix, due to their relatively remarkable various properties including abrasion resistance, optical properties, conductivity, flame retardance and widespread potential applications.

Although various attempts have been made to incorporate conductive nanofillers into the polymer matrix, there are still limitations in meeting the requirements of composite airframes. First, the resulting nano-hybrid composites cannot assimilate sufficient amount of the nanofiller to achieve the indispensable performance for surface protection [3]. Second, the viscosity of the matrix resin can dramatically increase after being mixed with the nanofiller, thereby negatively affecting the manufacturing process of the composite material [4]. Third, filtration of the nanofiller by the textiles during liquid molding of the composites leads to a non-uniform distribution of the nanofiller, which results in insufficient final protection of the whole aircraft structure [5].

This research focuses on CFRP surface protection via depositing a uniform and sufficient protection layer on CFRP surface through a liquid composite molding method to manufacture large-scale and complex aircraft structure in the future. In this study, graphene was selected as a nanofiller for reinforcement of polymers owing to its superior conductivity, friction performance, thermal stability and large specific surface area characteristics [6]. Specifically, high loadings of reduced graphene oxide (RGO, up to 0.2 g) were dispersed in a resin film by a ball mill-assisted dispersion technology. A percolating-assisted resin film infusion (RFI) method was proposed to enrich sufficient amounts of nanofiller on the composite surface while maintaining a uniform distribution in-plane.

* Corresponding author. Tel: +86 029 83399516. Fax: +86 029 82660114. E-mail address: ygduan@mail.xjtu.edu.cn (Yugang Duan)

2 EXPERIMENTAL

2.1 Materials

The epoxy matrix system used in this study was comprised of a bisphenol A epoxy resin (Epolam 5015, AXSON, France), a phenolic epoxy resin (Institute of Aeronautical Materials, China) and polyethersulfone (PES, Changchun Jilin University Special Plastic Engineering, China), while 4,4′-diamino-diphenylsulfone (DDS, Shanghai Experiment Reagent, China) was used as a hardener agent. RGO was obtained via oxidation of natural graphite flakes (according to the Hummers´ method [7]), followed by exfoliation of graphite oxide via ultrasonic treatment [8]. PAN-based 12 K carbon fibers arranged in a 300 g/m^2 areal weight unidirectional fabric (Toray Industries, Japan) was used as fiber reinforcements. All vacuum bagging materials were supplied by Sino-composite Co. Ltd.

2.2 Preparation

2.2.1 RGO dispersion in the resin film

First, a specific amount of RGO (0-0.2 g) was dispersed in a sealed breaker of acetone using a high intensity ultrasonic atomizer probe (40 kHz) at 60 ºC for 30 min. The suspension was separately added to the two types of epoxy resin (50 g) mentioned above and subsequently stirred at a rotational speed of 1000 rpm for 2 h to achieve the desired weight fraction of RGO in the epoxy resin. The resulted blend was further processed using a high-energy planetary ball mill (QM, Nanda Instrument, China) with three different types of zirconia balls (3, 6, and 11 mm in diameter). A total milling ball blend ratio of 5:1 was used in this ball milling process. To avoid severe destruction of the graphene structure, the rotating tray was controlled to provide a speed of 200 rpm [9]. Then, the resultant dispersion was degassed at 150 ºC by a vacuum pump for 12 h to remove acetone. After that, appropriate quantities of the prepared bisphenol A epoxy resin and PES were heated while stirring at 190 ºC until PES was completely dissolved in the epoxy. Then, another phenolic epoxy resin was mixed into the solution for 2 h, and the hardener agent was added while stirring at 120 ºC. The resultant solution was coated on a hot plate using the flow-casting method. After cooling to room temperature, a transparent resin film was obtained and a polyester film was adhered on the surface of the resin film for protection and operation.

2.2.2 Composite processing

The multi-scale reinforcement laminate was fabricated by the percolating-assisted RFI method, a schematic layout of which is shown in Figure 1 (a). The RFI method developed herein is advantageous in that it can reduce the relative flow distances to be overcome while also eliminating the need for a low viscous resin system [10]. In this process, the bleeder cloth, the peel ply, and the filter paper (1-4 μm) were first adhered on a heated mold in sequence. The as-prepared nano-hybrid resin film (150 mm x 150 mm) was placed on the filter paper, and then the fibrous preform was located (150 mm x 150 mm) in a stacking sequence of 0/90 added on its top. The preform edges were tightly sealed with sealant tape as dams to ensure the resin flow in the thickness direction. After that, the bagging arrangement was sealed with a vacuum bag and sealing tape.

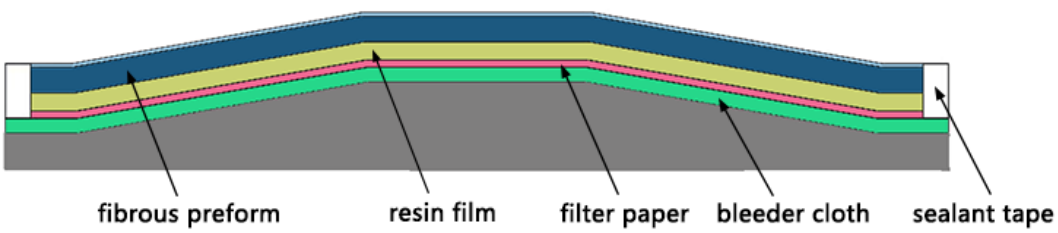

Figure 1. Scheme of the preform fabrication

As shown in Figure 3, the residual gas was removed by pulling a vacuum on the sealed preform. Secondly, the fibrous preform was heated up to 120 ºC for 1.5 h without vacuum while completely melting the resin films and the infuse amidst the fabric plies, and then the vacuum pressure was applied again. Thirdly, the prepared laminate was placed in an autoclave and post-cured for 4 h at 180 ºC and 2h at 200 ºC. The obtained composite was labeled as n-RGO/CFRP, where n stands for the mass of RGO in the resin film.

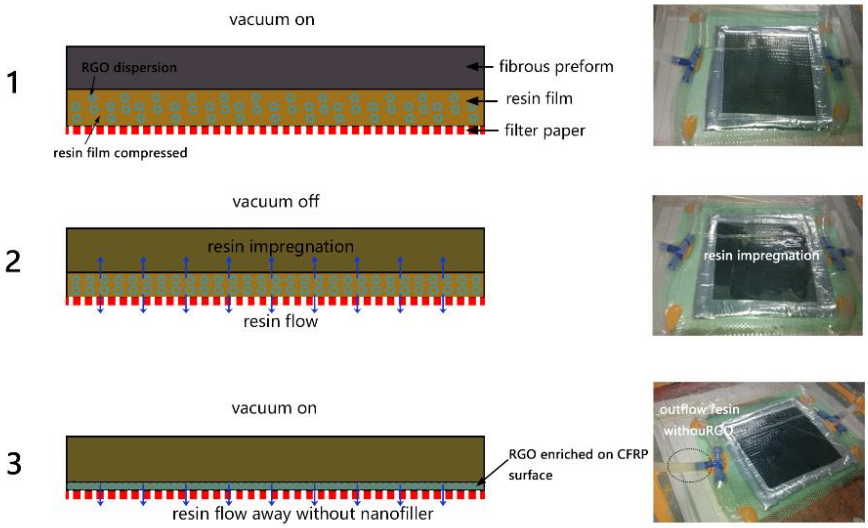

Figure 2. Schematic of the RFI processing to accumulate RGO on the CFRP surface and images of the RFI processing

2.3 Characterizations

The morphology of the CFRP was studied using field emission scanning electron microscopy device (Hitachi Su-8010, SEM, Japan) and an optical microscope (Leica DM 4000 M, German). After the simulated lightning strike test, an overhead view of samples was obtained by a digital camera (Nikon, D7200) and an ultrasonic scanning (D9500, Sonoscan, USA). To further examine the internal damage, a microfocus X-ray system (Y.Cheetah, YXLON, German) was used as a non-destructive ultrasonic inspection technique. The filtration effect was also investigated by identifying the spatial variations of the surface resistance using a four-point probe apparatus (1.56 mm of the inter-probe spacing), each data point was obtained as the average of five measurements.

An impulse lightning current of component A, as defined in SAE ARP-5412, was applied by using an impulse high-current generator (ICG, established by Xi'an Jiaotong University). This generator was capable of generating artificial lightning. Herein, an artificial lightning with a peak current of 40 kA with a waveform of 8/20 μs was utilized to inflict lightning damage to the samples. The electrical conductivity of CFRP was measured on rectangular sample using a multimeter (Keithley 2700). The surfaces of interest were polished with abrasive papers and subsequently painted with a suspension of silver in methyl isobutyl ketone (HUMISEAI 948-06G, USA) which allows good electrical contact between the surfaces of the sample and the copper electrodes.

The thermal degradation behavior of the composite panels was evaluated with cone calorimeter tests (FTT0007, UK) according to ASME E1354/ISO 5660. An external radiant heat flux of 50 kW/m^2 was applied. All of the panels were placed on a horizontal position and wrapped with a thin aluminum foil.

The friction and wear behaviors of the composite were performed using a friction tester (CFT-I, China). Composite panel (70 mm*50 mm*0.6 mm) were fixed on the guide of friction

plate, which moved back and forth with a constant speed of 0.1m/s. The dynamic friction coefficient were tested under the conditions of 200 N loading pressure whitin 6 min. The dynamic friction coefficient of the sample is calculated as follows:

$$u_d = \frac{M_D}{P R_{cp}} \quad (1)$$

Where u_d is the dynamic friction coefficient, M_D is the dynamic friction torque, P is the total pressure, R_{cp} is the sample width.

3 RESULTS AND DISCUSSION

3.1 Manufacture and surface conductivity control

The main purpose of the proposed method is to control the nano-filler introduction process so that it can be uniformly accumulated on the composite surface to provide the required surface protection. In this method, the filter paper and the sealant tape were proposed to form a confined region to limit the RGO flow along the thickness direction thereby avoiding the expansion of RGO from the preform (Figure 2). In this region, the dispersed RGO firstly permeated in the fabric with the resin impregnated, but it was gradually intercepted via two main filtration mechanisms namely cake filtration and deep bed filtration [4, 11]. Cake filtration takes place when the size of RGO is larger than the available pore size, resulting in the deposition of RGO within the fibrous medium. On the other hand, deep bed filtration is characterized by a gradual capture of the RGO with a size lower than the pore channels. Continuous capture of RGO through deep bed filtration can result in the reduction of the dimensions of the available flow channels leading to cake filtration at a microscopic level. Ultimately, all available flow channels or pores were gradually blocked by RGO. After impregnation, the excess resin was extracted from the fibrous preform. However, since only the resin can pass through the filter paper, RGO was completely percolated by the filter paper. Additionally, the filter paper can also decrease the flow rate of the resin, thereby reducing the flushing of the resin on the distribution of RGO while ensuring the maximum content of RGO on the composite surface [12]. As shown in Figure 3 (a), the inner surface of the filter paper was black (a1, a2), whereas the peel ply adhered to the filter paper was white (a3). These results indicated that this method can resolve the loss of nanofillers so that a sufficient amount of conductive nanofiller can be enriched on the composite surface for lightning protection. The typical morphology of the top surface of CFRP laminate after processing is shown in Figure 3 (b). RGO was fully covered on the surface, whereas the specimen prepared without filter paper remained clean and smooth indicating that RGO were pumped out and squeezed out from the preform (Figure 3 (c)). The cross-section view of CFRP laminate (Figure 6) further verifies RGO distribution in the laminate. RGO (0.05g) was gradually intercepted and infiltrated into the fibrous medium with the depth of 391 μm (Figure 6 (a)). In Figure 6 (b), a resin layer (31μm) consisting RGO was covered on the laminate indicating RGO can accumulate on the surface after flow channels of fibrous medium were blocked. Consequently, the gap between RGO was reduced with the resin pumped out, and RGO was overlapped with each other to form a crosslink network of conductivity ultimately.

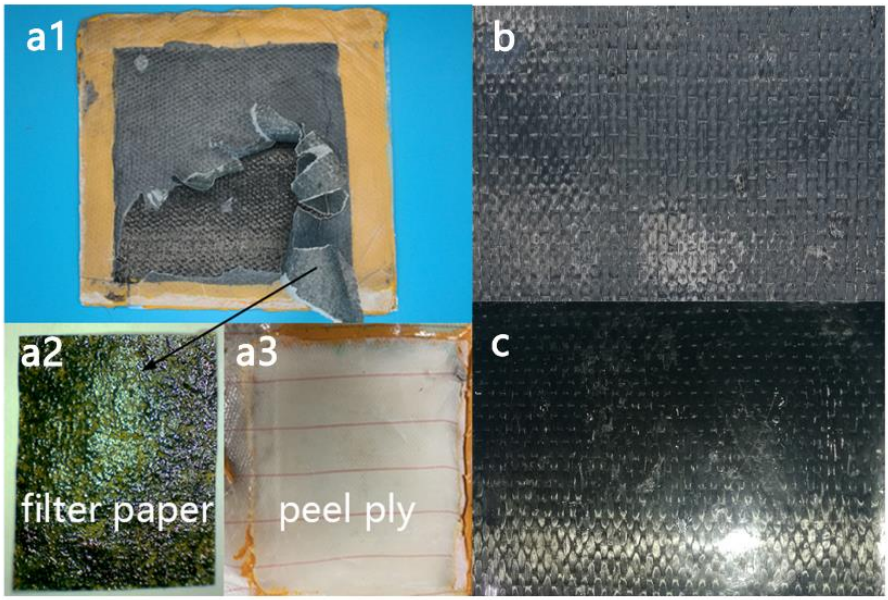

Figure 3. (a) Images of the prepared specimen (a1), filter paper (a2), and peel ply after curing (a3), and the typical morphology of the top surface of CFRP laminate prepared (b) with filter paper and (c) without filter paper

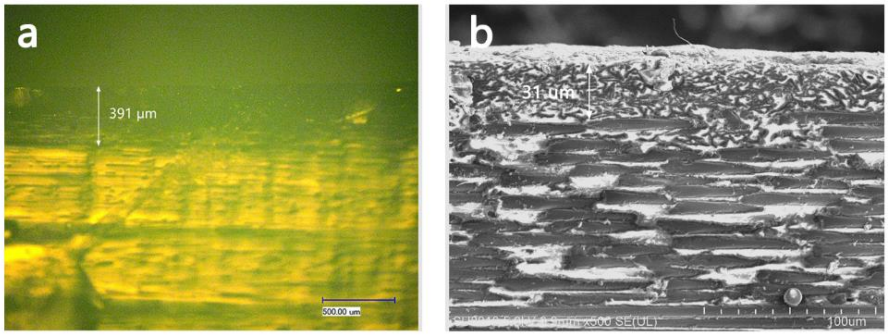

Figure 4. The cross-section view of the prepared sample by side-light transmission photomicrographs (a) and SEM image (b)

3.2 Lightning-strike tests

The amounts of conductive RGO required to improve the composite conductivity were determined by forming the conductivity network at volume fractions exceeding the percolation threshold. The electric conductivity results as a function of the mass of RGO in the resin film are shown in Figure 5 (a). Apparently, the in-plane conductivity was improved by increasing the RGO mass. At RGO loads up to 0.05 g, the in-plane conductivity sharply increased to 371 S/cm (the maximum conductivity was 440 S/cm for 0.2 g of RGO/CFRP), in other words, at RGO loadings of ca. 0.05 g, a very high fraction of electrons was permitted to flow through the composite upon lightning exposure owing to the creation of interconnecting conductive channels. Since conductive RGO was enriched on the laminate surface, this in-plane conductivity was much higher than that of nanofiller incorporating within CFRP (i.e., 120-140 S/cm for carbon nanotube grown on CFRP), thereby supposing a more effective protection for lightning strike. Another issue producing inadequate lightning protection is non-uniform distribution of the nanofiller, which accounts for the filtration effect during the molding process. In this method, the resin film containing RGO dispersed was forced to flow through the thickness direction of the fibrous preform. This direction is the shortest path for infiltration, thereby reducing the minimum required time of manufacture. While overspreaded

RGO were restrained between fibrous preform and filter paper, and flowed only in the thickness direction, thus not only guaranteeing the homogeneity of RGO in-plane, but also making sufficient amount of RGO on CFRP feasible. Moreover, the highly dispersion of RGO in the resin film is indispensable for homogeneous distribution as well. As shown in Figure 5 (b), the composite surface resistance was recorded as a function of the distance using a four-point probe, and the results for dispersed and undispersed RGO were compared. The fluctuation of the surface resistance of the highly dispersed composite was relatively modest as compared with the non-dispersed composite. In Figure 5 (c), RGO was homogeneously dispersed on the surface, which suggests that RGO forms a network structure to enhance the electrical properties of CFRP. Moreover, the reduction in the surface resistance was more significant for the highly dispersed system (Figure 5 (d)), which indicated that dispersed RGO facilitated the formation of a conductive network. As shown from Figure 5 (b), with regard to the anisotropy of CFRP, the resistance in the 0 direction was significantly lower than that in the 90 direction. However, when RGO was inserted, the resistance became identical in both directions. Since the conductivity of graphene is much higher than that of carbon fiber, the apparent surface resistance mainly consisted of that of RGO.

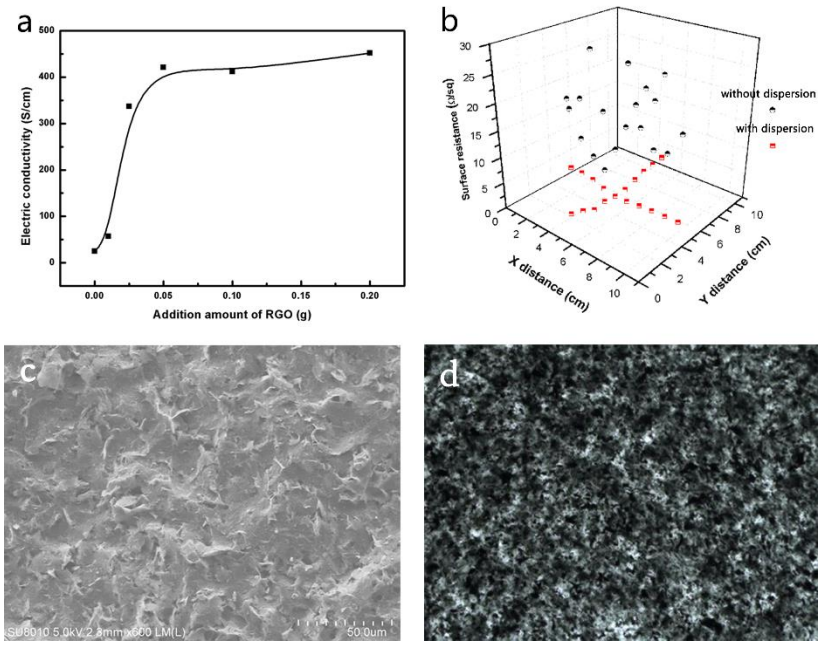

Figure 5. (a) In-plane electrical conductivity of RGO/CRFP; (b) surface resistance of dispersed and undispersed RGO/CRFP; (c) SEM images of the top surface; and (d) image of RGO dispersed in a resin film

The typical surface damage incurred by applying the simulated lightning current is shown in Figure 6. A top view of the composite at the site of the simulated lightning current attachment is also showed in Figure 8. Pristine CFRP tested at 40 kA (Figure 6 (a) and (c)) showed significant damages consisting of broken fibers as well as resin evaporation and deterioration. This significant damage was produced by the low conductivity of the composite which caused thermal energy build-up and subsequent the damage. A large area of the resin was degraded on the specimen surface, leaving the bare fiber yarns to the outside. However, the 0.05 g-RGO/CFRP specimen showed barely visible resin deterioration exclusively located around its center (Figure 6 (b) and (d)). In terms of the internal damage, CFRP showed a darker and larger sign region indicating extensive damage beyond the fiber damage and the resin deterioration area (Figure 7). From the cross section in the center of pristine CFRP, it can be confirmed that a major delamination took place on the first two layers with a

propagation direction along the 0/90 interface. However, the interval crack between the two adjacent became thinner and shorter after RGO modification, which indicated that the RGO protection can reduce the lightning strike damage.

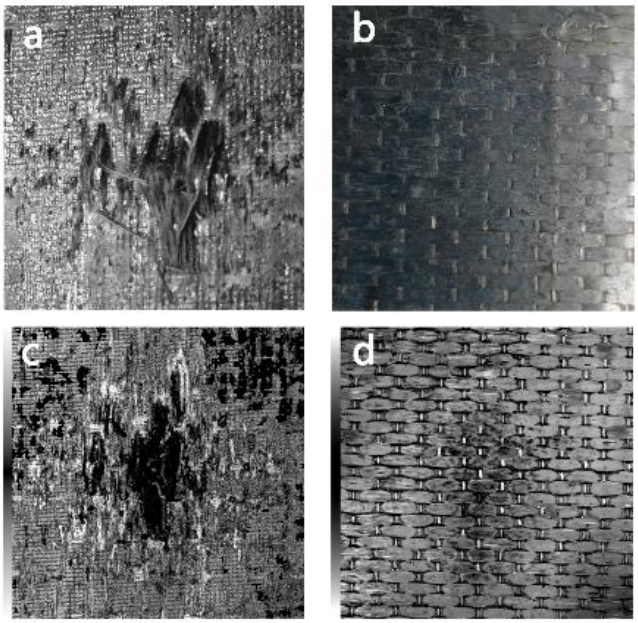

Figure 6. Surface damage images of: (a, c) CFRP and (b, d) 0.05 g-RGO/CFRP samples observed by digital camera (a, b) and C-scope inspection (c, d)

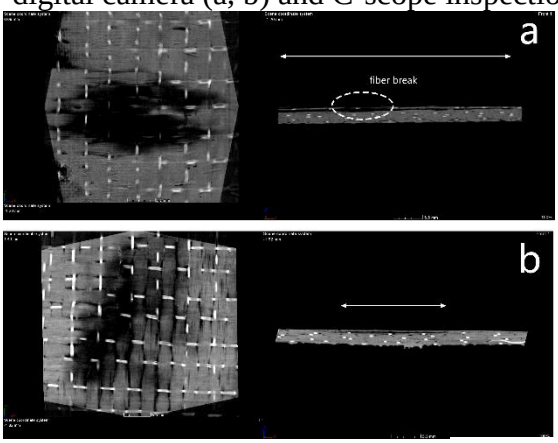

Figure 7. Internal damage images of: (a) CFRP and (b) 0.05 g-RGO/CFRP by X-ray inspection

3.3 Flame retardance

As shown in Figure 11, the thermal degradation behavior of CFRP was characterized by cone calorimetry. The heat release rate (HRR) curves of the RGO/CRFP (Figure 11 (a)) showed a similar trend as in the case of CFRP, whereas a reduction was observed for RGO/CRFP. The peak heat release rate of the RGO/CRFP composite was lower than that of CFRP, and gradually decreased with the amount of added RGO. The heat release curves also showed a delay in the time-to-peak HRR for RGO/CRFP as compared to CFRP. Obviously, the inserted RGO protection can restrict the thermal degradation and improve the resistance. A reduction in the mass loss during the combustion was obtained in the case of RGO/CFRP composites (Figure 11 (b)). The mass loss was mainly derived from the epoxy decomposition. Compared with CFRP, the total mass loss of RGO/CFRP decreased slightly with the amount of RGO, and ca. a 20 wt% of the resin matrix was lost during the test, whereas a 25 wt% was lost in the case of CFRP. This result demonstrated that the RGO protection on the CFRP can

improve its thermal resistance, thus preventing resin matrix from undergo pyrolysis.

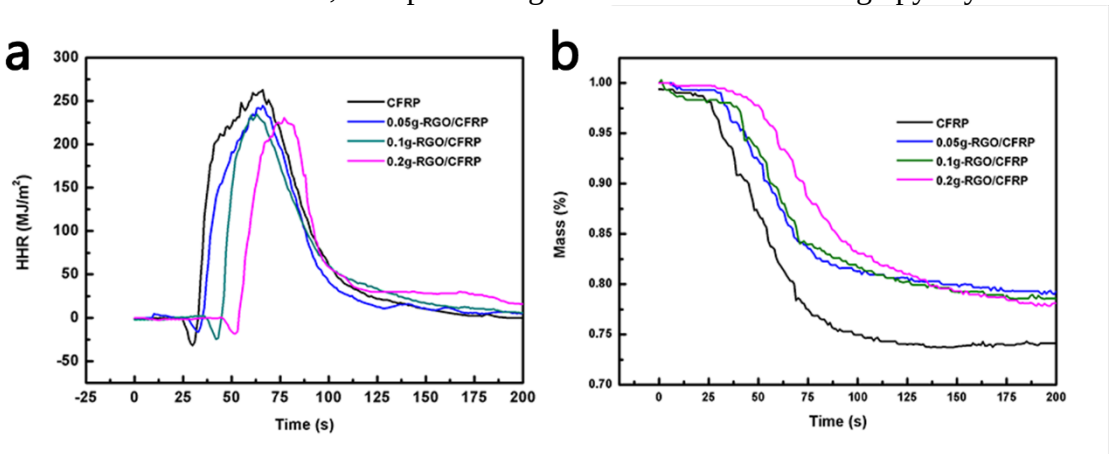

Figure 8. Comparison of (a) the heat release rate curves and (b) the mass loss for CFRP and 0.05 g-RGO/CFRP

3.4 Wear and friction

Figure 9 shows the dynamic friction coefficient of the CFRP tested by a running-in process test rig. It can be seen that the friction and wear behavior of CFRP was improved by introducing RGO. This reduction can be associated with the formation of a solid transfer layer when RGO inserted. With the formation of a uniform and tenacious transfer layer, sliding region occurs between the surface of the RGO layer and the counterpart, instead of the rough surface of the composite and the steel counterpart. The worn surface of the untreated CFRP was characterized by severe fibers cutting and lots of debris of fibers and resin matrix (Fig. 10). However, the worn surface was smoother and the adhesion and plough marks were nearly invisible after RGO inserted (Fig. 10 A1). Also, The CF were well bonded with the adhesive at the boundary of friction area (Fig. 10 B2), which indicates that the deposited RGO contributes to effectively protect CF, thus bore most of the load between the contact surfaces and obstructed the real contact area between the counterpart and CFRP, which significantly improve the tribological properties of CFRP composite.

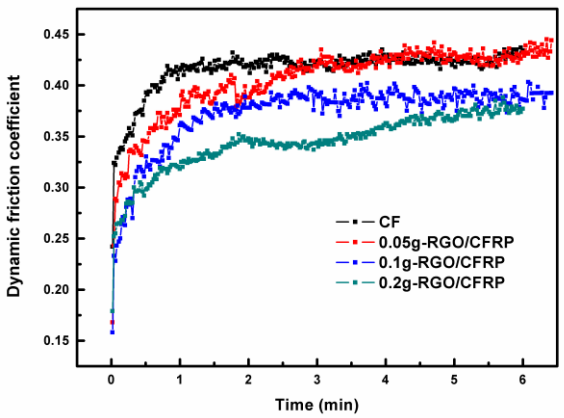

Figure 9. Variations of the dynamic friction coefficient of CFRP

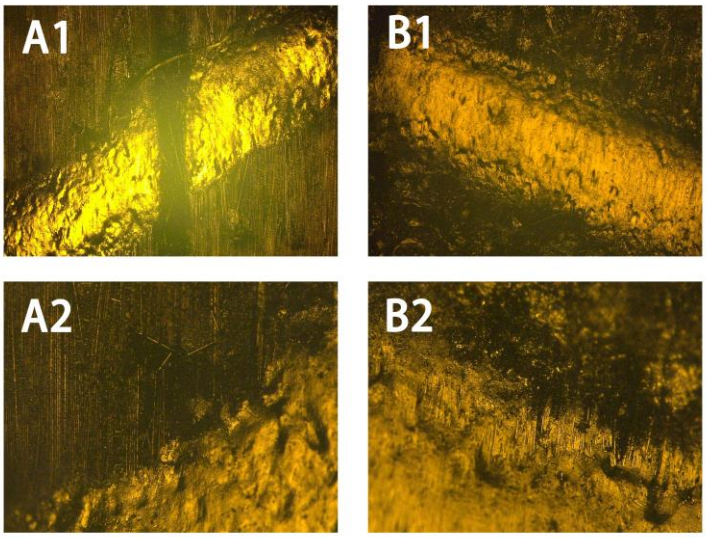

Figure 10. morphologies of the worn surface of CFRP

4 CONCLUSIONS

The results of this investigation demonstrated the feasibility of a developed RFI processing for multi-scale reinforced composites being formed by CFRP with RGO accumulated on its surface for lightning protection. Also, this developed RFI method can be applied to the integration molding of large-scale composite parts with a sufficient and uniform distribution of nanofiller, these factors limiting other approaches of multi-scale reinforced composites. Moreover, this method can maintain the mechanical properties of the fiber reinforced composite, while offering a new surface modification approach for additional applications such as flame retard, lightening striking and wear performance.

Acknowledgment

This research was supported by the NSFC of China [51275393] and [51275393], Xi'an Jiaotong University Funds of Fundamental Scientific Research [xkjc 2014010], and the Program for New Century Excellent Talents in University [NCET-11-0419].

Reference

[1] Hirano Y, Katsumata S, Iwahori Y, Todoroki A. Artificial lightning testing on graphite/epoxy composite laminate. Composites Part A: Applied Science and Manufacturing. 2010;41(10):1461-1470.

[2] Chivas-Joly C, Gaie-Levrel F, Motzkus C, Ducourtieux S, Delvallée A, De Lagos F, et al. Characterization of aerosols and fibers emitted from composite materials combustion. Journal of hazardous materials. 2016;301:153-162.

[3] Yokozeki T, Goto T, Takahashi T, Qian D, Itou S, Hirano Y, et al. Development and characterization of CFRP using a polyaniline-based conductive thermoset matrix. Composites Science and Technology. 2015;117:277-281.

[4] Wichmann MH, Sumfleth J, Gojny FH, Quaresimin M, Fiedler B, Schulte K. Glass-fibre-reinforced composites with enhanced mechanical and electrical properties–benefits and limitations of a nanoparticle modified matrix. Engineering Fracture Mechanics. 2006;73(16):2346-2359.

[5] Abliz D, Ziegmann G, Duan Y, Li D, Meiners D. Effect of CNT Concentration on Mechnical Properties of Composites Manufactured by Compression Resin Transfer Molding (CRTM). 16th EUROPEAN CONFERENCE ON COMPOSITE MATERIALS, Seville, Spain2014.

[6] Stankovich S, Dikin DA, Dommett GH, Kohlhaas KM, Zimney EJ, Stach EA, et al. Graphene-based composite materials. nature. 2006;442(7100):282-286.

[7] Schniepp HC, Li J-L, McAllister MJ, Sai H, Herrera-Alonso M, Adamson DH, et al. Functionalized single graphene sheets derived from splitting graphite oxide. The Journal of Physical Chemistry B. 2006;110(17):8535-8539.

[8] Tang L-C, Wang X, Gong L-X, Peng K, Zhao L, Chen Q, et al. Creep and recovery of polystyrene composites filled with graphene additives. Composites Science and Technology. 2014;91:63-70.

[9] Tang L-C, Wan Y-J, Yan D, Pei Y-B, Zhao L, Li Y-B, et al. The effect of graphene dispersion on the mechanical properties of graphene/epoxy composites. Carbon. 2013;60:16-27.
[10] Garschke C, Weimer C, Parlevliet P, Fox B. Out-of-autoclave cure cycle study of a resin film infusion process using in situ process monitoring. Composites Part A: Applied Science and Manufacturing. 2012;43(6):935-944.
[11] da Costa EFR, Skordos AA, Partridge IK, Rezai A. RTM processing and electrical performance of carbon nanotube modified epoxy/fibre composites. Composites Part A: Applied Science and Manufacturing. 2012;43(4):593-602.
[12] Ma L, Wu L, Cheng X, Zhuo D, Weng Z, Wang R. Improving the interlaminar properties of polymer composites using a situ accumulation method to construct the multi-scale reinforcement of carbon nanofibers/carbon fibers. Composites Part A: Applied Science and Manufacturing. 2015;72:65-74.